

# Selection of Wavelength Calibration Targets for the ACS Grism

---

A. Pasquali, N. Pirzkal, J.R. Walsh  
November 15, 2001

---

## ABSTRACT

*We discuss the criteria for the selection of wavelength calibration targets for the ACS grism to determine its dispersion and zero point. The primary requirement is for compact emission line sources. SLIM 1.0 simulations indicate that Galactic Wolf-Rayet stars are to be preferred to extragalactic Planetary Nebulae, since they can provide the wavelength calibration of both the 1<sup>st</sup> and 2<sup>nd</sup> grism orders with exposures shorter than 1 minute and are genuine point sources. Two selected targets, WR45 and WR96, were observed with NTT/EMMI at high spectral resolution (1.26 Å/pix) between 5000 Å and 1 μm. These spectra will be used as templates to identify the emission lines in the SMOV observations of the same objects using ACS, and to ultimately assess the on-orbit dispersion of the grism with an accuracy of 5% of the nominal dispersion.*

---

## Introduction

Simulations carried out for emission-line objects of varying size and position angle on the sky have shown (Pasquali et al. 2001) that the size of the source projected onto the dispersion axis smears out the spectral resolution of the grism, producing severe line blending for sizes larger than 2 pixels (0.1'' in the case of the WFC) and a major axis PA < 45° with the image X axis. This result poses important restraints in the planning of wavelength calibration observations, such as those foreseen for the SMOV tests and subsequent pipeline calibration. Wavelength calibration sources should thus have minimal spatial extension to allow sensitive determination of the dispersion and zero point in orbit.

## The selection criteria

To ensure an accurate wavelength calibration of the ACS grism, the targets have to meet the following requirements:

- Their luminosity allows for reasonably short exposure times ( $< 1$  orbit).
  - Their optical spectra present a significant number of emission lines.
  - No nebulosity is associated with the targets which would degrade the spectral resolution of the instrument and increase the local background.
  - Spectrophotometric variability (either intrinsic or induced by an eclipsing companion and by orbital motion) is negligible so that emission features can be identified at the same wavelength at any observational date.
  - Targets should not lie in crowded field to avoid contamination by nearby spectra.
  - Targets should be visible as long as possible (likely CVZ) to allow repeated HST visits.
- In the past, Planetary Nebulae have well served calibration purposes because of their rich emission-line spectrum and large population in the Galaxy and in the Local Group. In what follows, we will show that they do not satisfy the above criteria and that another class of sources has to be used to calibrate the ACS grism in wavelength.

## The traditional calibrators: Planetary Nebulae

Galactic Planetary Nebulae (PNe) are rarely compact (full size  $< 0.1''$ ) when imaged with HST and even when compact often have a low intensity halo. Therefore, the need for preserving the nominal spectral resolution of the ACS grism requires extragalactic PNe to be observed.

Ciardullo et al. (1989) and Jacoby & Ciardullo (1999) have extensively observed Planetary Nebulae in M31 and measured  $H\beta$  line fluxes and object sizes. From their samples, we have selected the brightest and more compact PNe to be simulated with SLIM. They are listed in Table 1. At the distance of M31 these objects appear point-like (i.e. sizes typically less than  $0.05''$ ) so that in our simulations their size is set by the instrumental PSF.

PN	RA (2000)	DEC (2000)	Log( $H\beta$ )	Size ( $''$ )
CJFN #1	00:42:46.1	41:16:40.9	-15.1	$< 0.1$
CJFN #31	00:44:08.6	41:24:52.8	-14.6	$< 0.1$
JC #57	00:40:15.3	40:24:13.0	-15.0	$< 0.1$

**Table 1.** A subsample of bright and compact Planetary Nebulae belonging to M31. CJFN and JC are for Ciardullo et al. (1989) and Jacoby & Ciardullo (1999), respectively.

We have adopted for the above targets the model spectrum of NGC 7009 (cf. Pasquali et al. 2001) scaled to the  $H\beta$  line fluxes of Table 1 and have run SLIM to generate 1200 s exposures (no CRSPLIT was applied) for both the WFC and the HRC. The simulated grism images include the background and read-out noise given by the ACS ETC. The

WFC grism stamp image is shown in Figure 1; it includes both the 1<sup>st</sup> and 2<sup>nd</sup> order spectra of CJFN #1, #31 and JC #57.

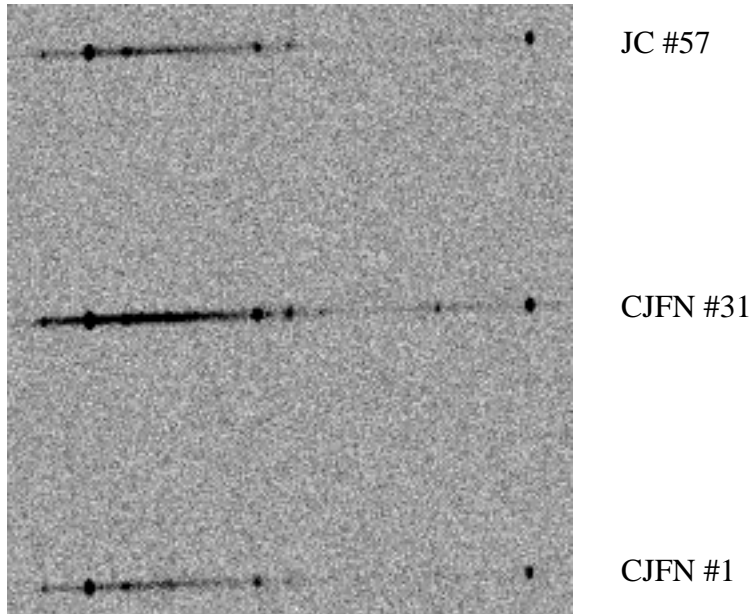


**Figure 1:** The 1<sup>st</sup> and 2<sup>nd</sup> order grism simulated WFC spectra.

The above spectra have been extracted with a box aperture 12 pixels (0.6'') wide and are presented in Figure 2, in units of count/pixel from the object position in the direct image. The background has not been subtracted; the subtraction however would not improve the S/N ratio since additional noise would be added.

For the adopted exposure time, none of the sample PNe provide a sufficient number of emission lines to wavelength calibrate the 2<sup>nd</sup> orders. As far as S/N is concerned, CJFN #31 and JC #57 are most suited in deriving the dispersion correction for the WFC grism 1<sup>st</sup> order and especially its zero point, although this takes almost half a HST orbit.

In the case of the HRC and accounting for the lower CCD QE and the higher spectral resolution than for the WFC, SLIM 2400 s exposures have been generated in order to achieve the same S/N ratio as for the WFC grism. Background and read-out noise have been added to the simulated grism image. The stamp image of the 1<sup>st</sup> and 2<sup>nd</sup> order spectra are shown in Figure 3.

The 45° tilt of the spectra requires an ad hoc extraction procedure, whereby the original grism image is rotated to align the dispersion axis with the image X axis and each spectrum is extracted with a box aperture of 5 pixels (0.14'') in the cross-dispersion direction. The resulting 1<sup>st</sup> and 2<sup>nd</sup> order spectra are plotted in Figure 4 in units of count/pixel from the object position in the direct image.

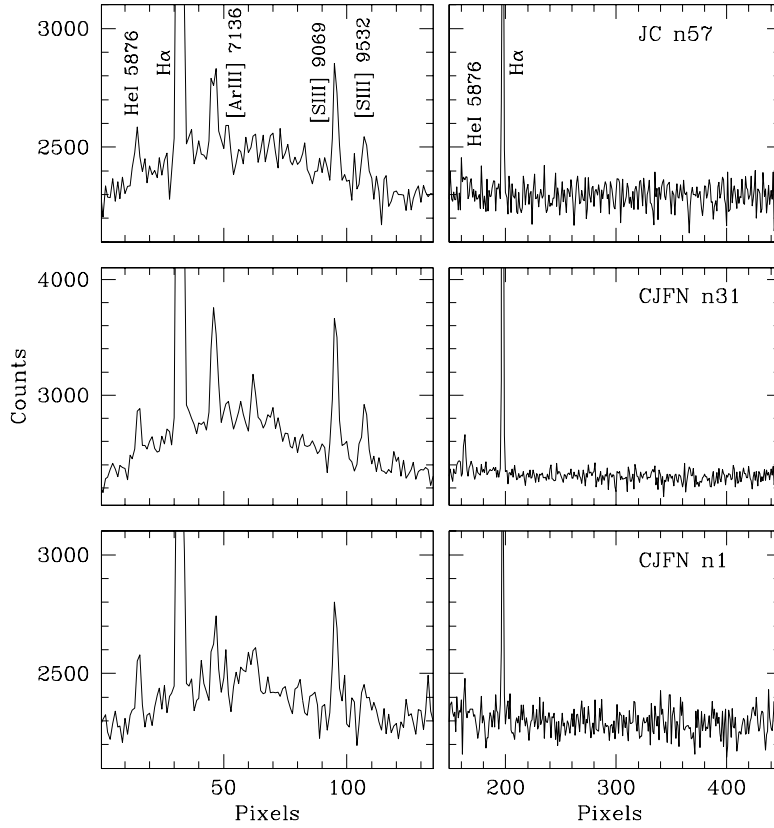


**Figure 2:** SLIM simulations of PNe in M31, as observed with the WFC grism in a 1200 s exposure. The 1<sup>st</sup> (in the left panels, at 40 Å/pix) and the 2<sup>nd</sup> order spectra (in the right panels, at 20 Å/pix) have not been background-subtracted.

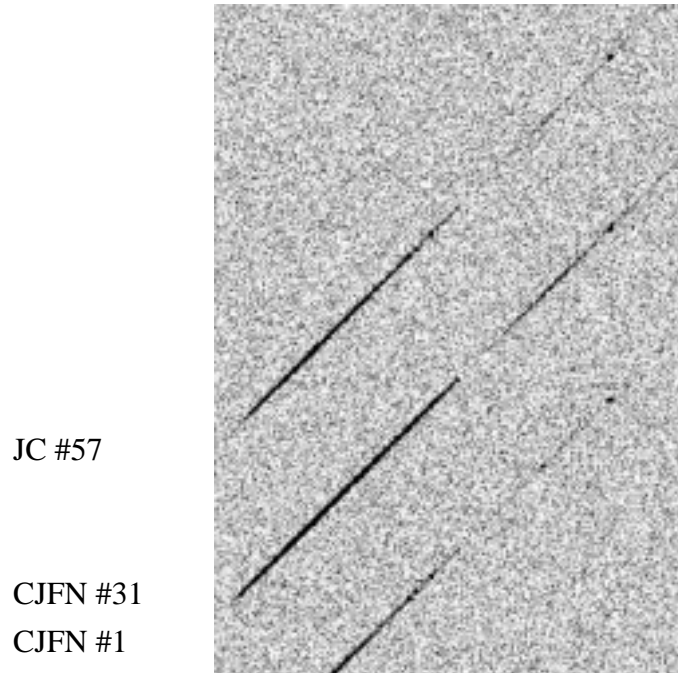


**Figure 3:** the 1<sup>st</sup> and 2<sup>nd</sup> order grism spectra simulated for the HRC.

Similarly to the WFC grism, PNe CJFN #31 and JC #57 can be used to determine the dispersion correction of the 1<sup>st</sup> order of the HRC grism, but this still requires a HST orbit integration. The 2<sup>nd</sup> orders are hardly detected.

In conclusion, observations of extragalactic PNe turn out to be too time-consuming for routine wavelength calibration and considering the number of orbits allocated to the SMOV grism tests. Moreover, extragalactic PNe can only be used to wavelength calibrate the 1<sup>st</sup> orders of the grism.

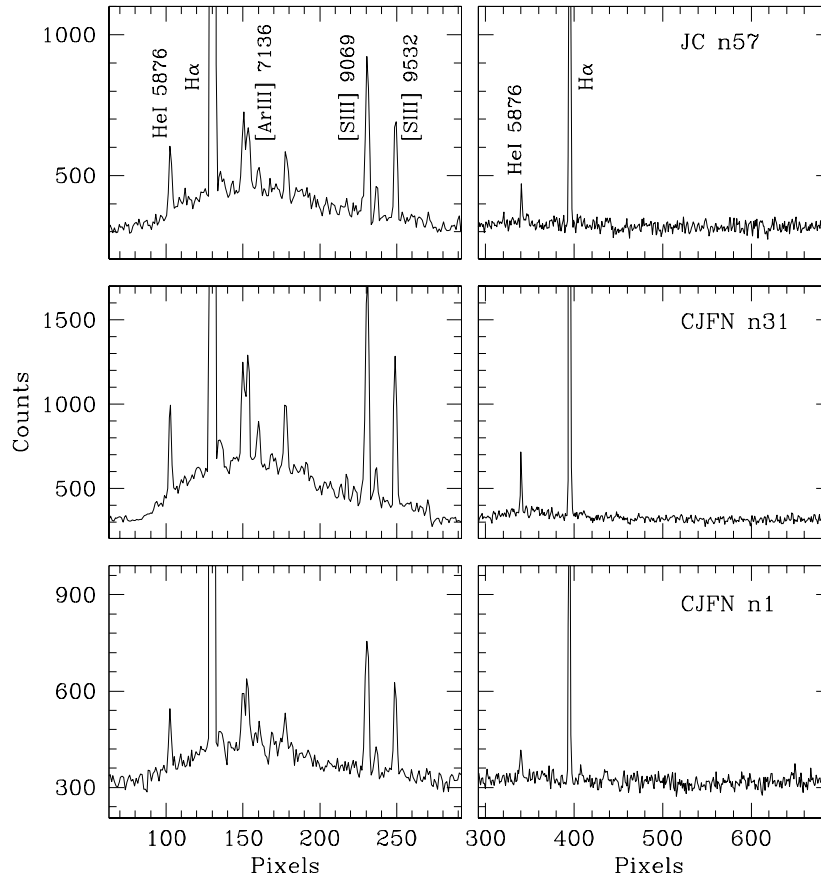


**Figure 4:** SLIM simulations of PNe in M31, as observed with the HRC grism in a 2400 s exposure. The 1<sup>st</sup> (in the left panels, at 25 Å/pix) and the 2<sup>nd</sup> order spectra (in the right panels, at 12 Å/pix) have not been background-subtracted.

In addition, the requirement to have multiple wavelength calibration spectra at different positions in the field, to measure the variation of the dispersion solution as a function of spatial position, cannot be met in one orbit for either the WFC or the HRC.

## An alternative choice: Galactic Wolf-Rayet Stars

The ACS spatial sampling and the spectral resolution of the grism suggest that the wavelength calibration be performed with point source emission line objects like Galactic Wolf-Rayet (WR) stars.

The spectrum of WR stars is characterised by a number of emission lines of H, He, N and C originating in the stellar wind. The predominance of either N or C features determines the classification of WRs into either WN or WC spectral types, respectively.

An example of these spectral classes is shown in Figure 5 (courtesy by P. Crowther).

The absorption at  $\lambda \sim 6250 \text{ \AA}$  is an artefact.

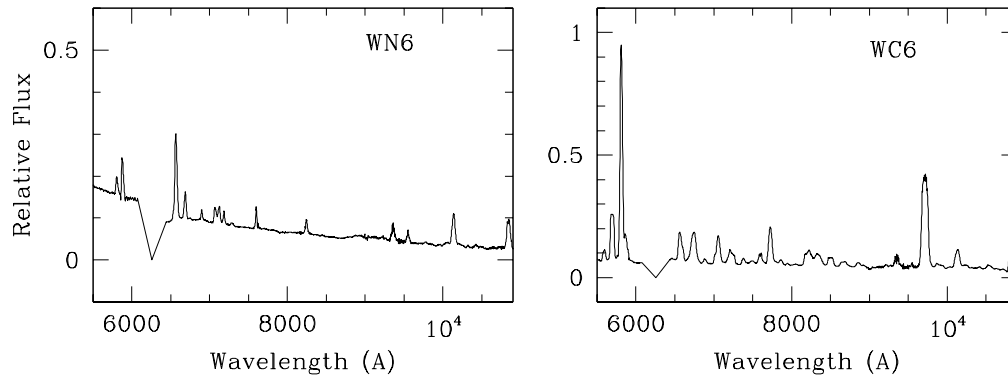


**Figure 5:** The optical spectra of typical WN6 and WC8 Wolf-Rayet stars.

WRs are known for their high velocity winds which considerably broaden their emission features. The line broadening produced by a wind speed of  $2000 \text{ km s}^{-1}$  in the case of the WFC and HRC grism is listed in Table 2, and has been computed with respect to the wavelength at which the 1<sup>st</sup> and 2<sup>nd</sup> order responses peak, which represents a mean value throughout the spectral range of the grism. The spectral resolution is  $40 \text{ \AA/pix}$  and  $20 \text{ \AA/pix}$  for the WFC 1<sup>st</sup> and 2<sup>nd</sup> order spectra,  $25 \text{ \AA/pix}$  and  $12 \text{ \AA/pix}$  for the HRC 1<sup>st</sup> and 2<sup>nd</sup> orders, respectively.

Line broadening	WFC grism	WFC grism	HRC grism	HRC grism
	1 <sup>st</sup> order $\lambda=7653 \text{ \AA}$	2 <sup>nd</sup> order $\lambda=5997 \text{ \AA}$	1 <sup>st</sup> order $\lambda=7005 \text{ \AA}$	2 <sup>nd</sup> order $\lambda=5999 \text{ \AA}$
in $\text{\AA}$	51	40	47	40
in pixels	1.3	1.9	1.9	3.3

**Table 2.** The line broadening induced by a stellar wind at  $2000 \text{ km s}^{-1}$  on the 1<sup>st</sup> and 2<sup>nd</sup> order spectra of the WFC and HRC grism. The wind “effect” has been computed for the peak wavelength of the 1<sup>st</sup> and 2<sup>nd</sup> order responses and is expressed in units of  $\text{\AA}$  and pixels along the dispersion axis.

According to Table 2, the stellar wind is hardly resolved in the 1<sup>st</sup> order spectra of both Channels, and partially affects the 2<sup>nd</sup> order spectra. van der Hucht (2001, The VII<sup>th</sup> catalogue of galactic Wolf-Rayet stars) lists a wind velocity range between  $\sim 700 \text{ km s}^{-1}$  and  $3300 \text{ km s}^{-1}$ , with 19% of the sample having a wind velocity larger than  $2100 \text{ km s}^{-1}$ . The mean wind velocity computed over the catalogue is  $(1730 \pm 700) \text{ km s}^{-1}$ .

Following the selection criteria listed in page 2, two WR stars have been first selected from the VII<sup>th</sup> Catalogue by van der Hucht which are listed in Table 3.

	Spectral type	RA (2000)	DEC (2000)	V	Wind velocity
WR45	WC6	11 38 05.2	-62 16 01	14.80	2100 $\text{km s}^{-1}$
WR96	WC9	17 36 24.2	-32 54 29	14.14	1100 $\text{km s}^{-1}$

**Table 3.** Basic parameters for the selected Wolf-Rayet stars.

Their finding charts follow in Figure 6; WR45 is on the left and WR96 on the right. The field of view is  $3' \times 3'$ .

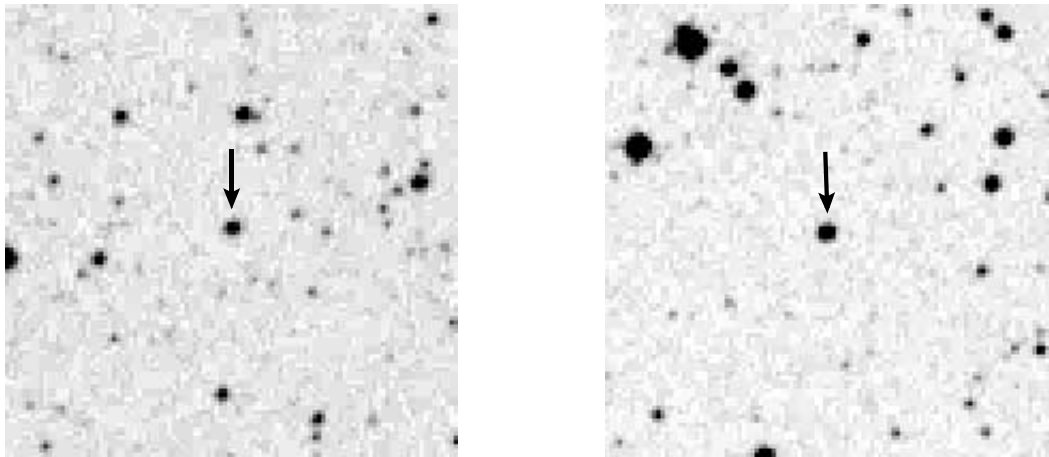


**Figure 6:** The finding charts of WR45 (on the left) and WR96 (on the right). The field of view is  $3' \times 3'$  (images from the Digital Sky Survey).

To overcome the lack of homogeneous spectra published for these objects over the grism wavelength range, we observed WR45 and WR96 with EMMI mounted on the ESO NTT telescope in June and August 2001. One hour of ESO Director General Discretionary Time was allocated to acquire spectra in the following ranges:

-  $5000 \text{ \AA} - 7500 \text{ \AA}$  at  $1.26 \text{ \AA/pix}$  (in REMD mode with Grating #8,  $\lambda_c = 6200 \text{ \AA}$ );

- 7300 Å - 9750 Å at 1.26 Å/pix (in REMD mode with Grating #8,  $\lambda_c = 8550$  Å);

- 4000 Å - 9000 Å at 2.7 Å/pix (in RILD mode with Grism #2).

The high resolution spectra have been used to accurately identify the He and C emission lines, while the low resolution data have been used to properly calibrate the spectra in flux.

The spectra at high resolution are plotted in Figure 6 for both WR45 and WR96.

SLIM 1.0 (Pirzkal et al. 2001) has been used to produce WFC and HRC grism images, using the NTT observed spectra, which also include the background and read-out noise.

The ESO spectra shown in Figure 7 have served as SLIM input spectra.

The WFC 1<sup>st</sup> order spectra (extracted with IRAF) are plotted in Figure 8, left column, for an exposure time of 10 s, while the right column shows the 2<sup>nd</sup> orders obtained with an integration time of 60 s. They are in units of count/pixel from the object position in the direct image. The spectra are background-subtracted.

Both targets provide a large enough number of emission lines to calibrate in wavelength both the 1<sup>st</sup> and 2<sup>nd</sup> orders of the WFC grism in exposures shorter than 1 minute.

The 1<sup>st</sup> and 2<sup>nd</sup> order spectra of WR45 and WR96 as observed with the HRC grism are found in Figure 9. They are plotted in units of count/pixel from the object position in the direct image. The 1<sup>st</sup> orders have been obtained by integrating for 20 s, while the 2<sup>nd</sup> order spectra have an exposure time of 60 s. Again, the number of emission features is large enough to allow an accurate wavelength calibration of both orders of the HRC grism within 1 minute exposure, thus allowing several dispersion measurements as a function of position on the chip with one orbit.

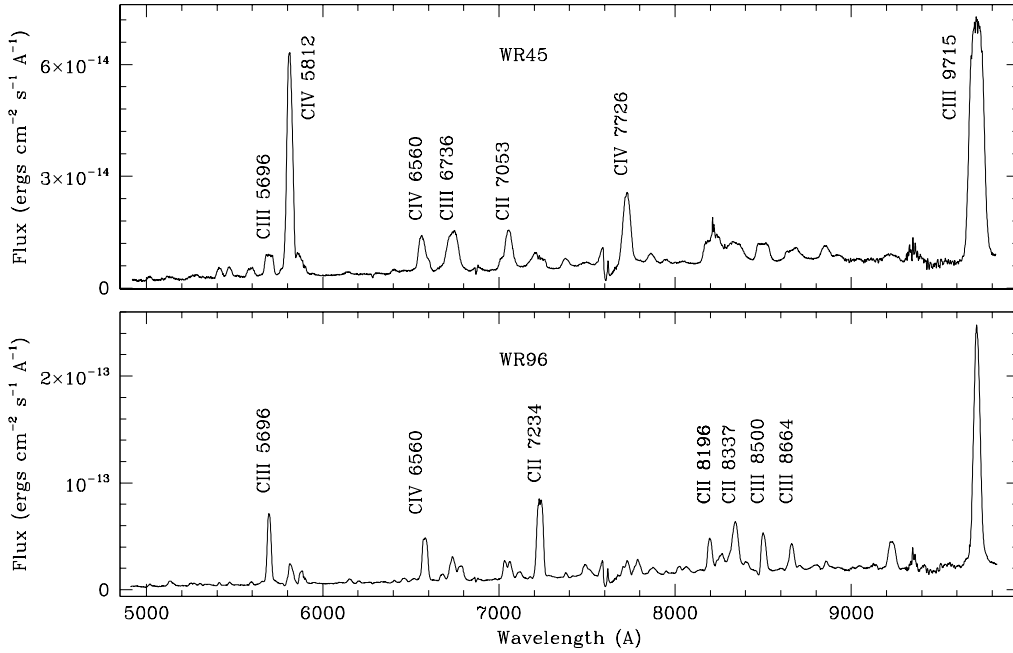


**Figure 7:** The high resolution (1.26 Å/pixel) spectra of WR45 and WR96 obtained with the NTT/EMMI spectrograph.

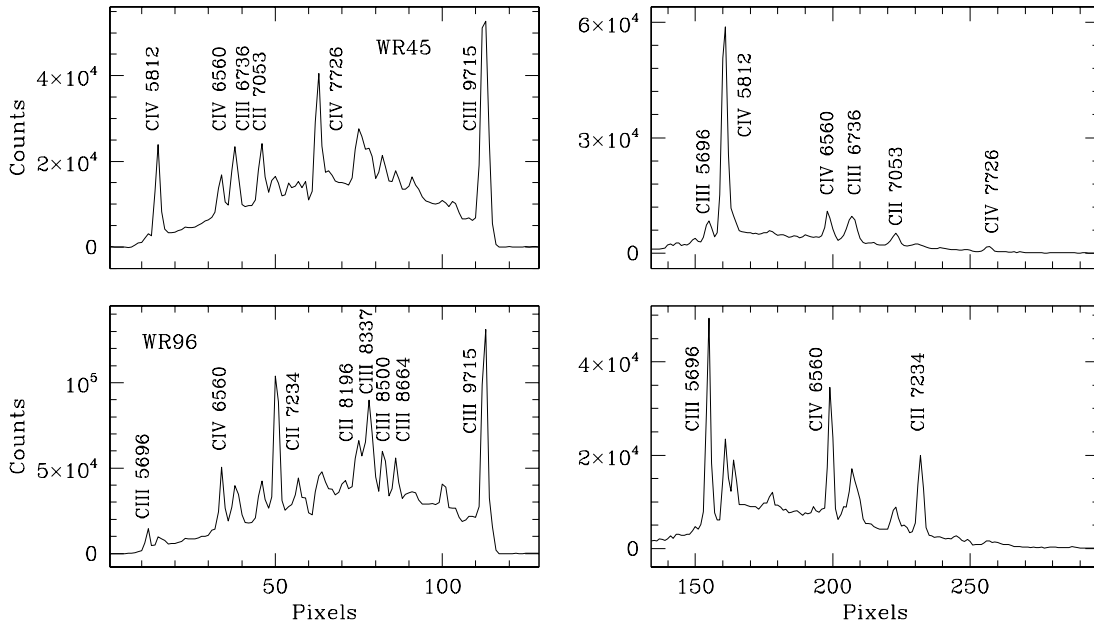


**Figure 8:** The SLIM output spectra for WR45 and WR96. First orders are plotted in the left column and refer to an exposure time of 10 s. The second order spectra are shown in the right column and have been computed for an integration time of 60 s.

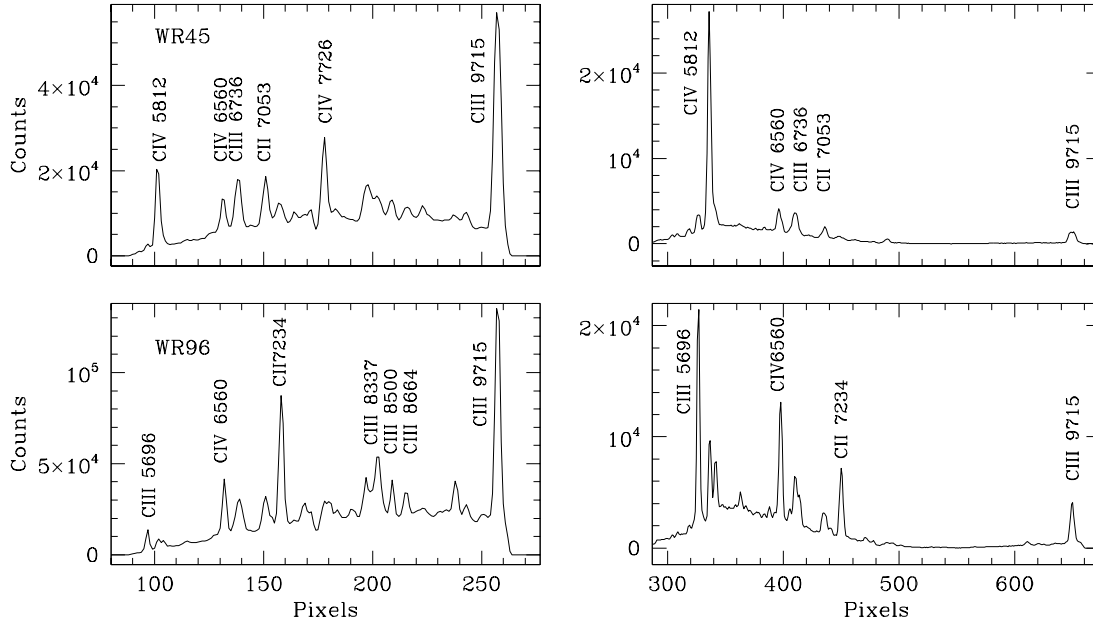


**Figure 9:** The SLIM output spectra for the HRC grism. 1<sup>st</sup> orders are plotted in the left column and refer to an exposure time of 20 s. The 2<sup>nd</sup> order spectra are shown in the right column and have been computed for an integration time of 60 s.

As a counter-check, we have derived the dispersion correction of the 1<sup>st</sup> and 2<sup>nd</sup> orders of the grism for both the WFC and the HRC. Specifically, we have measured the position of each identified line in the SLIM output for WR45 and WR96 in pixel scaled to the position of the object in the direct image, and fitted pixel against wavelengths with POLYFIT in IRAF, assuming a first order polynomial. The results, dispersion and zero-point of each grism order in each channel are listed in Table 4 as averaged values over the two simulated WRs. The RMS of the fits is 5% of the derived dispersion.

	WFC 1 <sup>st</sup> order	WFC 2 <sup>nd</sup> order	HRC 1 <sup>st</sup> order	HRC 2 <sup>nd</sup> order
Dispersion ( $\text{\AA}/\text{pix}$ )	39.91 +- 0.03	19.95 +- 0.01	25.02 +- 0.02	12.45 +- 0.03
Zero-point ( $\text{\AA}$ )	5219.04 +- 0.57	2606.56 +- 4.19	3273.41 +- 3.23	1629.51 +- 0.90

**Table 4.** The grism parameters: dispersion and zero-point, in the case of the WFC and the HRC. These values are averaged over the SLIM simulated spectra of WR45 and WR96.

## Conclusions

Proper wavelength “calibrators” for the ACS grism have to be compact sources, in non crowded fields. They should not show significant variability in line intensity and should be bright enough to allow the calibration of the 1<sup>st</sup> and 2<sup>nd</sup> order spectra of the WFC and HRC grism, using short exposure times such as those planned for the SMOV tests and anticipated for routine wavelength calibration.

In the case of ACS optical spectroscopy (i.e. with the WFC and HRC grism), SLIM 1.0 simulations have shown that extragalactic PNe (i.e. in M31), although compact enough not to be resolved by HST, are generally too faint to be calibration targets.

Galactic WR stars, which satisfy the above mentioned requirements, are alternative wavelength “calibrators”. Simulations of template WC spectra have shown that WC stars can be observed in less than 1 minute and provide a large number of emission lines at good S/N for the calibration of both 1<sup>st</sup> and 2<sup>nd</sup> grism orders, for both the WFC and HRC. As a result, two objects, WR45 and WR96, have been selected as main wavelength calibrators of the WFC and HRC grism.

## Acknowledgements

We would like to acknowledge the ESO Director General Discretionary Time programme and the NTT team who carried out the observations in servicing mode.

## References

Ciardullo, R., Jacoby, G.H., Ford, H.C., Neill, J.D., 1989, ApJ, 339, 53

Jacoby, G.H., Ciardullo, R., 1999, ApJ, 515, 169

Pasquali, A., Pirzkal, N., Walsh, J.R., Hook, R.N., Freudling, W., Albrecht, R., Fosbury, R.A.E., 2001, “The Effective Spectral Resolution of the WFC and HRC Grism”, ST-ECF ISR ACS 2001-002

Pirzkal, N., Pasquali, A., Walsh, J.R., Hook, R.N., Freudling, W., Albrecht, R., Fosbury, R.A.E., 2001, “ACS Grism Simulations using SLIM 1.0”, ST-ECF ISR ACS 2001-001

van der Hucht, K. A., 2001, “The VIIth catalogue of galactic Wolf-Rayet stars”, New AR, 45, 135